Effect of the Nucleation Mechanism on Complex Poly(L-lactide) Nonisothermal Crystallization Process. Part 1: Thermal and Structural Characterization

Andrea Martinelli, Massimo Calì, Lucio D'Ilario, Iolanda Francolini, Antonella Piozzi

Dipartimento di Chimica, Sapienza Università di Roma, P.le A. Moro 5, 00185-Roma, Italy

Received 30 October 2010; accepted 16 December 2010
DOI 10.1002/app.33978
Published online 11 April 2011 in Wiley Online Library (wileyonlinelibrary.com).

ABSTRACT: The effect of the holding temperature and time in the melt state of poly(L-lactide) (PLLA) samples on the nonisothermal melt crystallization process and on the structure have been investigated by means of DSC, polarized optical microscopy and wide angle X-ray scattering. As standard starting material, single crystals grown from dilute solution were used. In the mild melting condition, the survived athermal nuclei favor high temperature polymer crystallization, while the more severe treatment leads the PLLA to crystallize at higher supercooling with a sporadic nucleation. At the intermediate melting temperature a distinct double nucleation mechanism was observed while at the lower nuclei concentration, a double crystallization rate was also found.
 J Appl Polym Sci 121: 3368–3376, 2011

Key words: nucleation; differential scanning calorimetry (DSC); crystallization; polylactide; wide-angle X-ray scattering (WAXS)

INTRODUCTION

Poly(L-lactide) (PLLA) is a thermoplastic semicrystalline polyester widely investigated in recent years by many research groups. These studies may be roughly divided into two main topics. The first one deals with the polymer application in the biomedical field, since, beside its good mechanical properties, it can be completely degraded in non toxic products and resorbed when placed in contact with mammalian body fluids.[1] These features make it one of the selected materials for surgical implantations, drug delivery system and scaffolds preparation.[2–5] This technological and applicative research stimulated a deeper investigation on the polymer physicochemical properties (the second main topic). These two topics are strictly correlated each other because of the implication of the PLLA structure, morphology and crystallinity on the biodegradation rate, cell adhesion (namely, surface morphology and roughness) and mechanical properties. Beside this aspect, it was observed that PLLA shows *per se* some stimulating peculiarities which are still under investigation, dealing with the influence of the crystallization condition on the crystallization kinetics, crystal structure, and melting behavior.[6] In melt or cold crystallization experiments, mainly conducted in isothermal condition, it was observed a discontinuity in the following polymer properties when crystallized at temperature (T_c) upon or below about 100−120°C: spherulitic grow rate (G) and size, IR spectroscopic and thermal properties (DSC), wide and small angle X-ray scattering (WAXS, SAXS) profiles.[7–12] These findings were initially ascribed by some authors to the crystallization regime transition from II to III, as evidenced by the Hoffman-Lauritzen analysis on G versus T_c data, and, recently, to the effect of the crystallization temperature T_c on the polymer crystal structure.[13,14] In fact, it was observed that at $T_c \geq 120$°C PLLA crystallizes in the α form, consisting in two chains with 10_3 helical conformation packed into an orthorhombic cell with $a = 10.7$ Å, $b = 6.45$ Å, and $c = 27.8$ Å. Changes in lattice parameters were recorded at lower crystallization temperature and at $T_c < 90$–100°C PLLA was found to crystallize in the limit disordered α′ form, characterized by an hexagonal packing of the chains having the same 10_3 helical conformation as in the α form. At the intermediate temperature PLLA assumes a mixed α and α′ form. These differences in crystal structure can explain some of the peculiar characteristics of PLLA crystallization process, including the discontinuity at 120°C in the double bell-shaped curve of polymer crystal growth, the minimum long period observed at 120°C and the DSC exothermic peak at about 160°C recorded for sample crystallized

Correspondence to: A. Martinelli (andrea.martinelli@uniroma1.it).
Contract grant sponsor: MIUR.

at $T_c < 120°C$, due to the first order α′-to-α solid phase transition.[15]

The PLLA crystallization complexity was also observed in nonisothermal experiments which, occasionally, highlighted the presence of a not well resolved double melt crystallization. It has been tentatively attributed to the competition between the crystallization from survived crystal fragments (self-nuclei) and from spontaneous nuclei, to a generic change of the crystallization mechanism or to the transition from Regime I to Regime II, occurring during the nonisothermal crystal growth.[11,16–19] A univocal interpretation of the phenomenon is not possible, being different the experimental conditions used in the researches and lacking a systematic investigation.

It is well known that the tailored control of the primary nucleation mechanism in the polymer crystallization process gives the opportunity to directly modulate many polymer features. The presence, the concentration and the nature of nuclei in the polymer melt may, in fact, directly affect the supercooling at which the nonisothermal crystallization takes place and, indirectly, the transformation kinetics, the final sample crystallinity and morphology.

Therefore, in this study, by the proper choice of the standard starting polymer state and melting conditions, we were able to vary the concentration of self-nuclei and to explore a wide temperature range where the PLLA nonisothermal melt crystallization occurs. This allows us to enlighten the polymer transition complexity and to give an interpretation of the observed phenomena.

In particular, to adequately follow the effect of the melting condition, namely holding temperature (T_s) and time (t_s) of PLLA in the melt state, on the subsequent nonisothermal crystallization process, single crystals grown from dilute solution were chosen as standard starting material.[20] In fact, the solution crystallization offers the advantage:

- to completely erases the previous polymer thermal history and structure, avoiding the potential degradation of the polymer occurring in the melting process, usually used to prepare the starting standard state;
- to reduce the heterogeneous nuclei concentration which can interfere in the melt crystallization process;
- to obtain a highly reproducible and structurally well-characterized starting material;
- to explore the highest temperature range involved in the polymer melt memory effects. In fact, upon heating, the polymer lamellae melt and recrystallize in a thickened thermally stable structure, which melts at higher temperature.[21]

The PLLA nonisothermal crystallization process was followed by differential scanning calorimetry and polarized optical microscopy.

It was observed that the temperature range where the nonisothermal crystallization takes place during controlled cooling (5°C min^{-1}) undergoes a large variation, passing from about 140°C, when the thermal treatment is mild and the athermal nuclei survives in the melt (self-nucleation region or Domain II, according to Fillon et al. definition), to about 115°C, when the severe melting condition is sufficient to erase the former crystalline memory and homogeneous nucleation occurs (homogeneous melt region or Domain I).[22] At the intermediate thermal treatment a double crystallization process was observed: at low athermal nuclei concentration the sporadic nucleation begins before the sample reaches the complete crystallization with predetermined mechanism. Moreover, at the lowest self-nuclei concentration, the transition slows down and moves toward the temperature region ($T \sim 120°C$) where the aforementioned change in the crystallization kinetics occurs. In these conditions the crystallization from predetermined nuclei shows a double DSC exothermic peak. The effect of the nonisothermal crystallization temperature, as ruled by nucleation mechanism, on the PLLA structure was analyzed by wide angle X-ray scattering (WAXS).

EXPERIMENTAL

Sample preparation

Poly(L-lactide) (PLLA, $M_n = 99000$, $M_w = 152{,}000$) was supplied by Fluka. It was first purified by solubilization in chloroform, filtration and precipitation with methanol. Single crystals were isothermally grown at $T_c^{sol} = 75°C$ (±0.5°C) from 0.25 wt/vol % polymer solution in *p*-xylene. PLLA was dissolved in 20% aliquot of solvent and then poured in the remaining fraction, preheated at the crystallization temperature. After 24 h the precipitated material was filtered and washed with aliquots of fresh solvent at T_c^{sol} and repeatedly washed at room temperature with ethanol to completely remove *p*-xylene. The samples were then dried in vacuum. The melting behavior of PLLA single crystals was followed by DSC measurement carried out at 10°C min^{-1} (Fig. 1).

PLLA self-nucleation and thermal analysis

The nonisothermal crystallization process was followed by differential scanning calorimetry and polarized optical microscopy.

A Mettler DSC822^e differential scanning calorimeter (DSC) was used for the thermal analysis. The

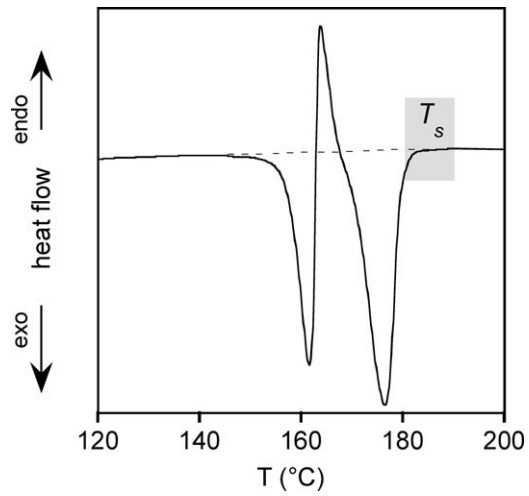

Figure 1 DSC thermogram of PLLA single crystals grown from *p*-xylene dilute solution at $T_c^{sol} = 75°C$, recorded at 10°C min^{-1}.

instrument was calibrated for the heat flow and temperature according to the standard procedures suggested by Mettler.

The DSC scans were performed on about 3 mg of PLLA single crystals sealed in aluminum pans under nitrogen atmosphere. The samples were first heated at 10°C min^{-1} above the melting temperature and hold at a dwelling temperature (T_s) in the range 180–190°C for 5 min. For the samples treated at 187°C a holding time $0 \leq t_s \leq 45$ min was also analyzed. According to literature results, both T_s and t_s were chosen so as to avoid or minimize degradation phenomena. The sample was then cooled at 5°C min^{-1} to 25°C to record the crystallization process.

Polarized optical microscopy

Polarized optical microscopy (POM) analysis was performed by means of an Optiphot2-Pol light microscopy (Nikon) equipped with a Linkam HFS 91 hot stage (Linkam) driven by a Linkam TP 92 temperature controller and connected to an image acquisition and analysis system. All the experiments were carried out under N_2 flow. The temperature was calibrated by following the melting of benzoic acid ($T_m = 183.5°C$) and succinic acid ($T_m = 122°C$). The samples were prepared by evaporating on glass cover slip PLLA single crystals suspension in ethylic ether to form a homogeneous powder thin layer. The glass cover slip, usually pressed upon the sample, was not used to avoid chain orientation effect during the polymer melting.

The obtained thermal analysis results were interpreted according to the definition of Fillon et al.,[22] who rationalized the temperature influence on self-nucleation (SN) by dividing the temperature at which the sample was dwelled in the melt state into three zones, according to the polymer behavior in the subsequent nonisothermal melt crystallization.

In experiments carried out on isotactic polypropylene Fillon et al. observed that:

- the thermal treatment at temperature just above the upper limit of the melting endotherm peak (Domain I) assures the complete polymer melting process and, during the sample cooling, in absence of "foreign" heterogeneous nuclei, sporadic nucleation occurs. In this conditions the polymer crystallizes at the higher supercooling;
- at lower temperature (Domain II or SN region) the melting is incomplete and the concentration of self-nuclei strongly affects the crystallization temperature. The thermal treatment into Domain II provides spherulites that may display the typical "granular structure," due to the orientational memory of the original crystalline lamellae;
- at the lowest melting temperature range (Domain III or annealing region), the large unmelted polymer fraction undergoes crystal perfection (annealing) and the crystallization takes place at the highest temperature through the formation of spherulites just superimposed to those present in the starting sample.

Wide angle X-ray scattering

Wide angle X-ray scattering (WAXS) experiments were carried out by using the Italstructures Imaging Plate Diffractometer IPD3000 operating at 40 KV and 30 mA with a monochromatic CuK_α radiation. The transmitted diffraction patterns, stored in a cylindrical imaging plate, were digitalized by a Cyclone Den Optix QST (Gender) scanner. The digitalized image was processed by using the MAUD software.[23] The camera geometry was calibrated with silicon powder.

RESULTS AND DISCUSSION

In Figure 1, where the DSC melting profile of PLLA single crystals grown at $T_c^{sol} = 75°C$ is reported, three peaks may be identified: a lower temperature melting process at 162°C followed by a distinct exotherm at 164°C and an upper temperature melting at 176°C. Such a behavior was assigned to the melting of original metastable PLLA crystals that recrystallize in a thicker structure during the heating, melting at the higher temperature.[21]

The shadowed zone in Figure 1 represents the temperature range (T_s) at which the polymer was dwelled in the melt state before the non isothermal

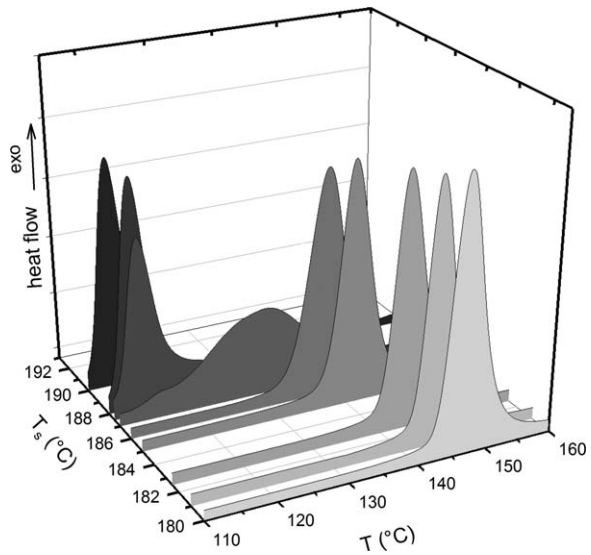

Figure 2 DSC cooling thermograms of PLLA samples held in the melt state at the different temperature T_s.

crystallization. POM observations showed that in this temperature region no macroscopic birefringent structures survive.

After the melting process was carried out at different T_s for 5 min, the PLLA samples were cooled at 5°C min^{-1}. The recorded thermograms are displayed in Figure 2.

As it may be seen, the thermal treatment has a significant effect on the crystallization process.

Between $T_s = 180$°C and $T_s = 186$°C the DSC profiles show only one exothermic peak, at a temperature defined as high crystallization temperature (T_c^H), that progressively moves from 146 to 139°C. As the dwelling temperature increases further a dramatic evolution of the crystallization process takes place. In particular, at $T_s = 187$°C the main peak undergoes a marked broadening and shifts at 132°C, while a shoulder appears at about 115°C, defined as lower crystallization temperature (T_c^L). At only 0.5°C above ($T_s = 187.5$°C) the higher temperature peak develops in a broad hump, approximately located at 126°C, and a distinct band appears at 114°C, remaining the only exothermic transition at higher T_s (188°C and 190°C).

In Figure 3, where T_c^H and T_c^L are reported as a function of the dwelling temperature, the presence of a transition temperature range $187 \leq T_s \leq 187.5$°C at which an abrupt crystallization mechanism change occurs is clearly evidenced.

To interpret the phenomena enlighten in the DSC experiment and to define the Domain limits according to the definition of Fillon et al.,[22] polarized optical microscopy observations were carried out to follow the spherulite evolution during the crystallization process. The same thermal treatment used in DSC measurement was employed. Figure 4 shows three representative image acquired at an intermediate crystallization stage after the polymer was melted for 5 min at temperature below ($T_s = 182.5$°C), upon ($T_s = 190$°C) and in correspondence of the previously mentioned transition zone ($T_s = 187$°C).

At $T_s = 182.5$°C, the spherulites have the same dimensions and the contact boundaries are linear [Fig. 4(A)]. It means that in this condition the crystalline structures started to grow at the same time, i.e., a predetermined nucleation mechanism was occurring. The wide size distribution of spherulites observed at $T_s = 190$°C, on the contrary, suggests a prevailing sporadic nucleation [Fig. 4(C)]. The sample dwelled in the melt state at 187°C shows an intermediate behavior, displaying larger spherulites with the same dimension, born in the early crystallization stage, together with smaller ones, grown later on [Fig. 4(B)]. This crystallization process is due to a mixed sporadic and predetermined nucleation mechanism.

In the T_s range we have explored, we never observed the granular structure reported in reference, due to the orientational memory of the original crystalline lamellae, nor the annealing process of the large unmelted crystal fraction, typical of the Domain III, probably occurring at lower T_s.[22]

During crystallization the formation of birefringent crystalline phase within the spherulites brings about an increase of the average transmitted light intensity of the POM images [$I(T)$] in the presence of crossed polarizers.[24] The overall crystallization process may then be conveniently followed by recording the $I(T)$ during the cooling scan, normalized according to

$$X_{POM}(T) = \frac{I_i - I(T)}{I_i - I_f} \quad (1)$$

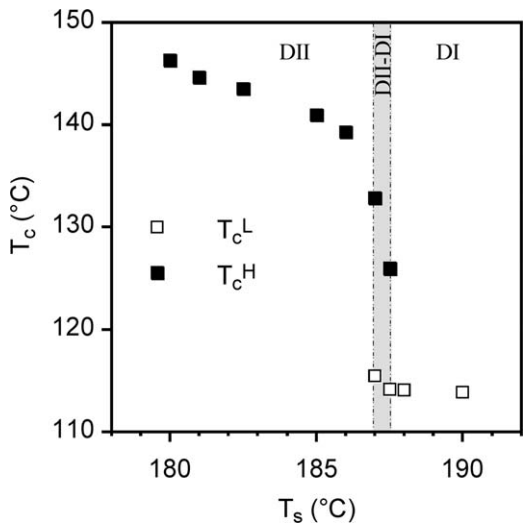

Figure 3 Effect of the dwelling temperature T_s on the nonisothermal crystallization temperature.

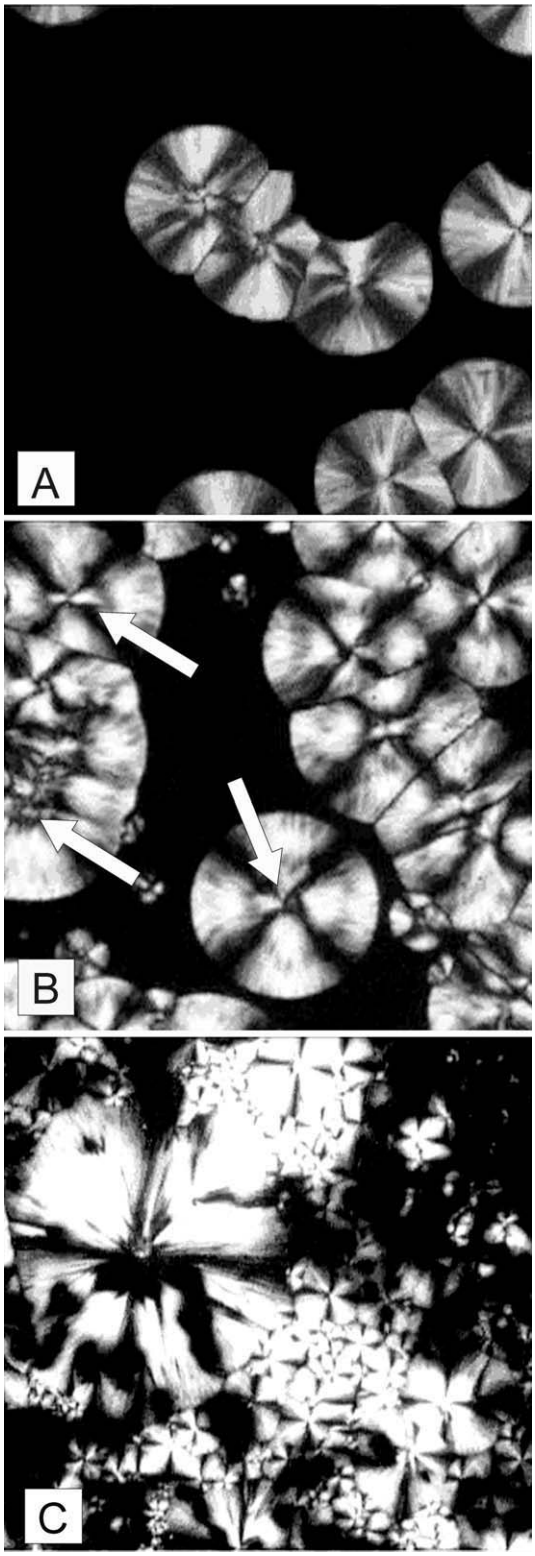

Figure 4 Polarized optical microscopy images acquired at an intermediate nonisothermal crystallization stage after the polymer was melted for 5 min at $T_s = 182.5$°C (A), $T_s = 187$°C (B), and $T_s = 190$°C (C).

where $X_{POM}(T)$ is the crystalline conversion degree, as followed by POM analysis, and I_i and I_f the initial and final transmitted intensity before and after the crystallization process, respectively. To compare the POM and DSC results, $X_{POM}(T)$ was reported in Figure 5 together with the crystalline conversion degree $X_{DSC}(T)$ obtained from calorimetric experiments reported in Figure 2 and defined as the ratio between the partial crystallization enthalpy recorded at the generic temperature T and the total crystallization enthalpy.

It is interesting to notice the good correlation between the two techniques, which could adequately describe the PLLA overall crystallization process, even when, at the intermediate dwelling temperature ($T_s = 187$°C), a double transformation takes place. The deviation at about 140°C between the two profiles recorded at $T_s = 187$°C is presumably due to the limited sample amount analyzed with the POM technique. The higher value of $X_{POM}(T)$ is due to the spherulites grown in the early crystallization stage, marked by arrows in the micrograph of Figure 4(B), and contributed to the initial sudden intensity increase.

After all, the PLLA behavior change as a function of the thermal treatment in the melt state may be ascribed to the different nucleation mechanism that governs the nonisothermal crystallization. At the lower T_s ($T_s \leq 186$°C), the ordered domains survived in the melt act as self-nuclei and the polymer crystallizes at lower supercooling. In this self-nucleation temperature region (Domain II, DII in Fig. 3), the T_c^H decrease with T_s is due to the progressive active nuclei concentration reduction. In the more severe T_s conditions ($T_s \geq 188$°C), 5 min are sufficient to destroy most of the active nuclei and sporadic nucleation occurs only at higher supercooling (Domain I, DI in Fig. 3). At the intermediate T_s ($187 \leq T_s \leq 187.5$°C) the well resolved mixed nucleation

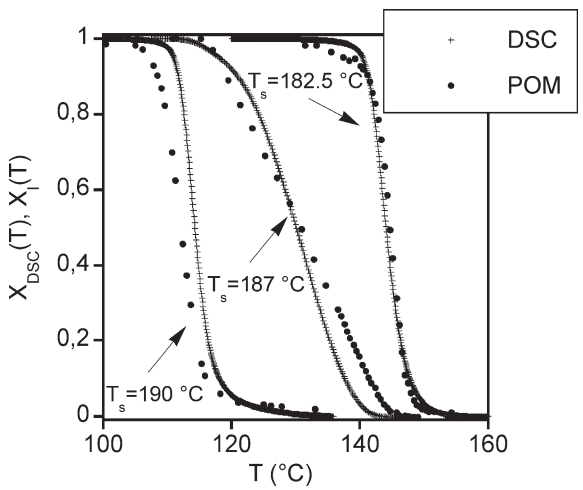

Figure 5 DSC and POM crystalline conversion degree ($X_{DSC}(T)$ and $X_{POM}(T)$) as a function of temperature for PLLA samples held at $T_s = 182.5$, 187, and 190°C recorded at 5°C min^{-1} cooling rate.

mechanism leads to a double spherulite population grown from predetermined and sporadic nuclei. On the ground of the Domains' definition, based on the polymer crystallization behavior, a superimposition of the Domains I and II occurs in the transition zone (DII+DI in Fig. 3). As anticipated, the Domain III is probably located at lower dwelling temperature and cannot be evidenced in the explored T_s range.

In general, it was observed that the sample starting standard state used in self-nucleation experiments has a great influence on the polymer crystallization behavior. Our results show remarkable differences respect to those found in SN experiments carried out by using melt-crystallized PLLA as standard starting sample, not exclusively imputable to the different polymer molecular weight used in the two researches.[25] Although the thermal treatment used to prepare the standard starting sample does not greatly affects the temperature range where the nonisothermal crystallization takes place (T_c), the Domain I upper temperature limit increases from 183°C, for melt crystallized starting sample, to 188°C, for our single crystals. Moreover, in our experiment we observed T_c steep decreases in correspondence of the Domain II-Domain I boundary region, whereas a linear decrease of T_c versus T_s is reported by Schmidt and Hillmyer.[25]

The phenomena observed in our experiments let us suppose that, as the T_s approaches the Domain II upper temperature limit, there is a selection of few stable self-nuclei coming from the former homogeneous crystalline structure, characterized by a narrow size distribution, which abruptly disappear at 188°C. In this condition, the great difference in the temperature dependence between the PLLA spherulitic growth rate [$G(T)$] and nucleation rate [$\dot{N}(T)$], the low concentration of "foreign" heterogeneous nuclei, characteristic of our single crystals sample, favor the appearance of the double crystallization process. In the light of the present observations it is possible to infer that the partially superimposed crystallization process observed in nonisothermal experiments and evidenced in a number of paper[11,16–19] as a peak shoulder at about 110–120°C before the dominant crystallization peak, is primarily related to a different nucleation mechanism activated at different temperature, as hypothesized by Wang and Mano[16]. It means that in PLLA nonisothermal crystallization the temperature range in which the transformation takes place is directly determined by the nucleation stage, that, on the other hand, indirectly influences the kinetics of the process and the final sample structure.

The overall crystallization enthalpy (ΔH_c), calculated from the thermograms of Figure 2, decreases with increasing the dwelling temperature (Fig. 6). This trend is opposite to that found by Wang and Mano, who investigated a higher melting temperature range (200–210°C).[16] These authors observed a ΔH_c increase with the severity of the melting treatment and they attributed it to the reduction of the polymer molecular weight.

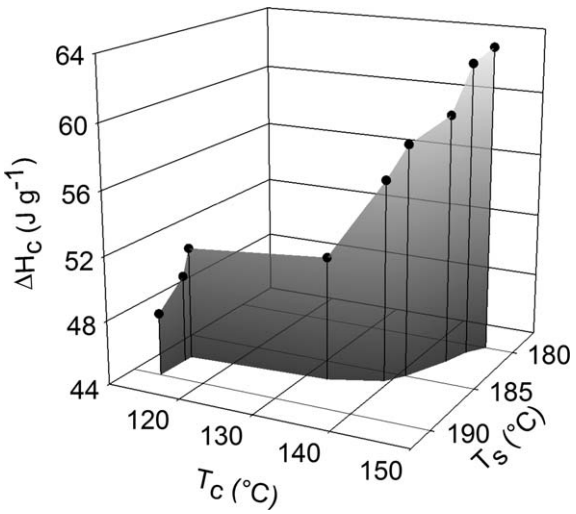

Figure 6 Effect of the dwelling temperature (T_s) and of the crystallization main peak temperature of Figure 2 (T_c) on the total crystallization enthalpy ΔH_c.

In Figure 6, the crystallization enthalpy is also reported as a function of the crystallization temperature T_c, taken at the maximum of the main exothermic peak of Figure 2. In the $133 \leq T_c \leq 146$°C range, corresponding to a holding temperature between 187 and 180°C, the sample crystallinity increases with the crystallization temperature. Similar effects of the crystallization temperature on PLLA crystallinity were reported by a number of authors.[6,8] In the plot of Figure 6 it is also possible to observe that, although the crystallization peak of the $T_s = 188$ and 190°C samples is fixed at $T_c = 114$°C, ΔH_c decreases at the higher holding temperature. This phenomenon, being independent from the T_c, evidences a direct correlation between the sample crystallinity with the melt history. It is probably due to the increase of chain entanglement concentration in the polymer melted at the higher T_s, which, in the following crystallization process, partially obstacles the neat structure set up.[20]

To investigate if the ordered structure survival is determined by thermodynamic or kinetic effects, experiments at different holding time t_s were carried out in the transition temperature range. It was found that it is sufficient just a $t_s = 1$ min at $T_s = 188$°C (data not reported) to completely destroy all the athermal nuclei and, hence, to observe the crystallization at T_c^{L} (Fig. 3). The situation for the holding temperature just in the middle of the transition zone of Figure 3 appears more complex. In Figure 7 A the crystallization DSC profile obtained by cooling at

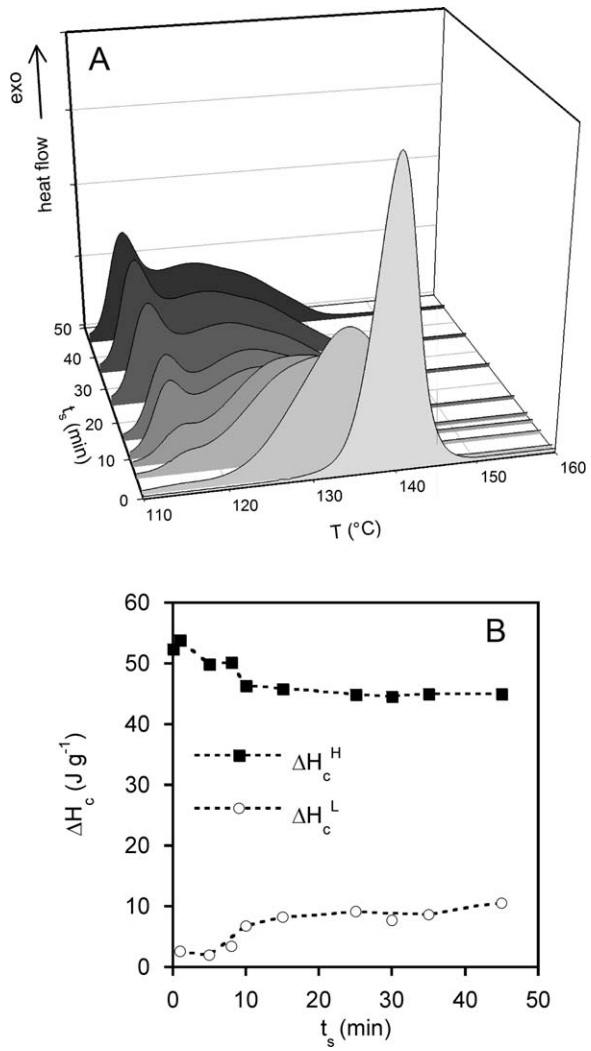

Figure 7 A: DSC crystallization thermogram evolution of PLLA samples dwelled at $T_s = 187°C$ for different dwelling time t_s. B: Effect of dwelling time t_s on high and low temperature crystallization enthalpy ΔH_c^H and ΔH_c^L, calculated by fitting the thermograms of Figure 7(A) with two or three Gaussian functions (see the text).

5°C min^{-1} the samples held at 187°C for different time t_s are reported.

In the first 10 min the thermograms show a clear evolution from a predetermined to a mixed predetermined and sporadic nucleation. From $t_s = 10$ min to $t_s = 45$ min no marked changes in the exothermic peak positions and intensities is observed. The crystallization enthalpy of the high and low temperature transition (ΔH_c^H and ΔH_c^L) was obtained by fitting the thermogram at $t_s = 5$ min with two Gaussian functions. For $t_s \geq 8$ min, a good DSC curve fit was reached with the sum of three Gaussian functions, one for the lower temperature process (ΔH_c^L, sporadic nucleation mechanism) and two for the higher temperature one (ΔH_c^H, predetermined nucleation mechanism). This last splitting is due to the fact that, because of the low concentration of predetermined nuclei, the PLLA crystallization slows down and takes place in the temperature region where the well-known rate discontinuity at 120°C occurs, already described in the Introduction section of this article.

Figure 7(B), where the effect of dwelling time t_s on high and low temperature crystallization enthalpy ΔH_c^H and ΔH_c^L is reported, shows that while the total crystallization enthalpy remains almost constant ($\Delta H_c^{tot} = 55 \pm 2$ J g^{-1}), the ΔH_c^H decreases and ΔH_c^L increases with t_s, till their values seem to level off from 10 to 15 min. All the results reported in Figure 7 imply that a thermodynamic temperature limit exists below which an equilibrium concentration is reached of ordered structures surviving after the higher melting temperature, where the DSC baseline is recovered after the melting endotherm. A more detailed discussion about the nuclei nature will be presented in the second part of this article.

The wide temperature range, at which the polymer is forced to crystallize according to its thermal history, has direct consequence on the PLLA structure.

As described in the Introduction section of this article, the PLLA can assume different structures according to the crystallization temperature. At $T_c \geq$ 120°C PLLA crystallizes in the α form, consisting in two chains with 10_3 helical conformation packed into an orthorhombic cell with $a = 10.7$ Å, $b = 6.45$ Å, and $c = 27.8$ Å. Changes in lattice parameters were recorded at lower crystallization temperature and at $T_c <$ 90–100°C PLLA was found to crystallize in the limit disordered α′ form, characterized by an hexagonal packing of the chains having the same 10_3 helical conformation as in the α form. At the intermediate temperature PLLA assumes a mixed α and α′ form.

So, according to the thermal history, and hence to the nucleation mechanism, we observed that the crystallization process could take place in different temperature ranges, above or below 120°C, that is in the α or α + α′ phase stability regions, respectively, (see Fig. 3). This situation gives rise to an indirect effect of the thermal treatment on the polymer structure, as verified by X-ray diffraction experiments. In Figure 8 the WAXS profiles of PLLA samples nonisothermally crystallized from $T_s = 182.5°C$ ($T_c^H =$ 145°C) and $T_s = 190°C$ ($T_c^L = 114°C$) are displayed. The diffraction patterns are normalized to the overlapped (200) and (110) reflection intensity.

As reported by Kawai et al., Zhang et al., and Pan et al.,[14,15,26] the differences in the peak position and intensity are due to the different crystal modifications. The α form of the $T_s = 182.5°C$ sample ($T_c >$ 120°C) is evidenced by the high intensity of the (103), (101), and (210) reflections and by the position of the (016) and (206) peaks at 23.9° and 24.9° and of

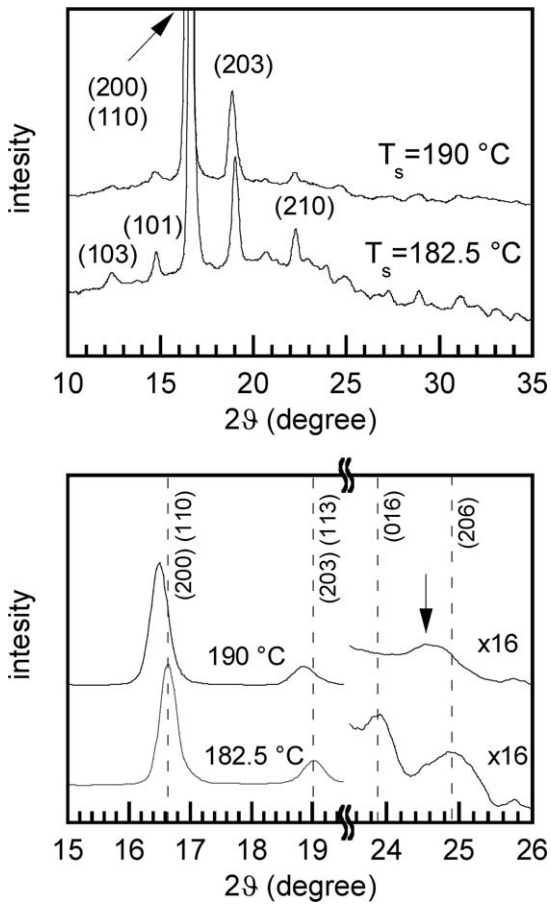

Figure 8 WAXS profiles of nonisothermally crystallized PLLA sample after being melted at $T_s = 182.5$ and 190°C for 5 min.

the superimposed (200)–(110) and (203)–(113) reflections at 16.7° and 19.0°, respectively. The $T_s = 190$°C sample, because of its lower crystallization temperature ($T_c < 120$°C), shows the features characteristic of a mixed α and α′ phase: the reflections at 12.4°, 14.7°, and 22.2° are very weak and the superimposed (200)–(110) and (203)–(113) peak positions shift at 16.5° and 18.8°, respectively.[14,15,26] Moreover, the characteristic (206) reflection of the α′-crystal can be clearly observed at $2\vartheta = 24.9°$.[26]

These results show that the crystalline structure is univocally determined by the crystallization temperature, which, in turn, is defined by the nucleation mechanism, depending on the severity of the thermal treatment.

CONCLUSIONS

In the present article the nonisothermal melt crystallization of PLLA single crystals was investigated as a function of the polymer holding temperature (T_s) and time (t_s) in the melt state by DSC, optical microscopy and WAXD measurements. To avoid polymer degradation and to follow the evolution of the PLLA in the melt state, we explored a temperature range just few degrees above the melting temperature.

According to the severity of the polymer thermal treatment in the melt state, the subsequent nonisothermal crystallization process was observed to follow three paths:

1. At the lower melting temperature ($180 \leq T_s \leq 186$°C, $t_s = 5$ min), residual ordered domains act as athermal nuclei and a single crystallization process via a predetermined nucleation mechanism was observed between 146°C and 139°C;
2. As the holding temperature increases ($187 \leq T_s \leq 187.5$°C, $t_s = 5$ min), a mixed predetermined and sporadic nucleation mechanism occurs, as evidenced by a distinct double crystallization process at about 130°C and 115°C, observed by DSC and POM analysis. According with the definition proposed by Fillon et al., in this temperature range a superimposition of Domain I and Domain II occurs.
3. At $T_s \geq 188$°C and $t_s = 5$ min, all the ordered structures disappear and a single crystallization process from sporadic nuclei takes place at high supercooling (114°C).

Moreover, it was observed that at $T_s = 187$°C the double nucleation mechanism persists for long dwelling time. From $t_s = 0$ min to 10 min the DSC crystallization peak intensity at the higher temperature decreases while the lower temperature one increases. The two process level off at about $t_s = 10$–15 min, implying that there is a thermodynamic temperature limit below which an equilibrium concentration of ordered structures survives after the higher melting temperature is reached.

WAXD analysis showed that the structure of the nonisothermal melt crystallized sample depends on its thermal history. In fact, the sample forced to crystallize at higher temperature by a predetermined nucleation ($T_s = 182.5$°C) shows the typical α phase diffraction pattern. The lower crystallization temperature necessary for the sporadic nuclei formation brings about a more disordered sample, characterized by the coexistence of the α and α′ phases.

References

1. Lee, J.-W.; Gardella, J. A., Jr. Anal Bioanal Chem 2002, 373, 526.
2. Zhang, X.; Mattheus, A.; Goosen, F. A.; Wyss, S. P.; Pichora, D. Polym Rev 1993, 33, 81.
3. Zhang, Z.; Feng, S.-S. Biomaterials 2006, 27, 262.
4. Martinelli, A.; Francolini, I.; D'Ilario, L.; Piozzi, A. Macromol Rapid Comm 2007, 28, 1900.

5. Zhu, Y.; Gao, C.; Liu, Y.; Shen, J. J Biomed Mater Res A 2004, 69, 436.
6. Lin, X.; Spruiell, J. E. J Polym Sci Part B: Polym Phys 2006, 44, 3378.
7. Di Lorenzo, M. L. Polymer 2001, 42, 944.
8. Zhang, J.; Duan, Y.; Sato, H.; Tsuji, H.; Noda, I.; Yan, S.; Ozaki, Y. Macromolecules 2005, 38, 8012.
9. Iannace, S.; Nicolais, L. J Appl Polym Sci 1997, 64, 911.
10. Salmeron Sanchez, M.; Gomez Ribelles, J. L.; Hernandez Sanchez, F.; Mano, J. F. Thermochim Acta 2005, 430, 201.
11. Pan, P.; Zhu, B.; Kai, W.; Dong, T.; Inoue, Y. J Appl Polym Sci 2008, 107, 54.
12. Cho, T.-Y.; Strobl, G. Polymer 2006, 47, 1036.
13. Hoffman, J. D.; Davis, G. T.; Lauritzen, J. I. In Treatise on solid state chemistry; Hannay, N. B., Eds.; Plenum Press: New York, 1976; Vol. 3, Chapter 7, p 565.
14. Kawai, T.; Rahman, N.; Matsuba, G.; Nishida, K.; Kanaya, T.; Nakano, M.; Okamoto, H.; Kawada, J.; Usuki, A.; Honma, N.; Nakajima, K.; Matsuda, M. Macromolecules 2007, 40, 9463.
15. Zhang, J.; Tashiro, K.; Tsuji, H.; Domb, A. J Macromolecules 2008, 41, 1352.
16. Wang, Y.; Mano, J. F. Eur Polym Mater 2005, 41, 2335.
17. Zhou, Z.; Ruan, J.; Zhou, Z.; Zou, J. Acta Phys-Chim Sin 2007, 23, 647.
18. Di Lorenzo, M. L. Eur Polym Mater 2005, 41, 569.
19. Pan, P.; Kai, W.; Zhu, B.; Dong, T.; Inoue, Y. Macromolecules 2007, 40, 6898.
20. D'Ilario, L.; Martinelli, A.; Piozzi, A. J. Macromol Sci-Phys 2002, B41, 47.
21. Fujita, M.; Doi, Y. Biomacromolecules 2003, 4, 1301.
22. Fillon, B. J.; Wittmann, C.; Lotz, B.; Thierry, A. J Polym Sci Part B: Polym Phys 1993, 31, 1383.
23. Lutterotti, L.; Bortolotti, M.; Ischia, G.; Lonardelli, I.; Wenk, H.-R. Z Kristallogr Suppl 2007, 26, 125.
24. Tsuji, H.; Takai, H.; Saha, S. K. Polymer 2006, 47, 3826.
25. Schmidt, S. C.; Hillmyer, M. A. J Polym Sci Part B: Polym Phys 2001, 39, 300.
26. Pan, P.; Zhu, B.; Kai, W.; Dong, T.; Inoue, Y. Macromolecules 2008, 41, 4296.